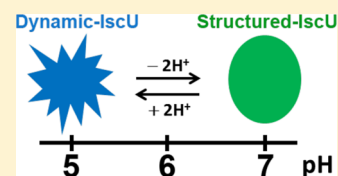


pH-Induced Conformational Change of IscU at Low pH Correlates with Protonation/Deprotonation of Two Conserved Histidine Residues

Ziqi Dai,^{†,§} Jin Hae Kim,^{‡,||} Marco Tonelli,^{‡,§} Ibrahim K. Ali,[‡] and John L. Markley^{*,†,‡,§}

[†]Biophysics Graduate Program, [‡]Biochemistry Department, and [§]National Magnetic Resonance Facility at Madison, Biochemistry Department, University of Wisconsin–Madison, Madison, Wisconsin 53715, United States

ABSTRACT: IscU, the scaffold protein for the major iron–sulfur cluster biosynthesis pathway in microorganisms and mitochondria (ISC pathway), plays important roles in the formation of [2Fe–2S] and [4Fe–4S] clusters and their delivery to acceptor apo-proteins. Our laboratory has shown that IscU populates two distinct, functionally relevant conformational states, a more structured state (S) and a more dynamic state (D), that differ by *cis/trans* isomerizations about two peptidyl-prolyl peptide bonds [Kim, J. H., Tonelli, M., and Markley, J. L. (2012) *Proc. Natl. Acad. Sci. U.S.A.*, 109, 454–459. Dai Z., Tonelli, M., and Markley, J. L. (2012) *Biochemistry*, 51, 9595–9602. Cai, K., Frederick, R. O., Kim, J. H., Reinen, N. M., Tonelli, M., and Markley, J. L. (2013) *J. Biol. Chem.*, 288, 28755–28770]. Here, we report our findings on the pH dependence of the D \rightleftharpoons S equilibrium for *Escherichia coli* IscU in which the D-state is stabilized at low and high pH values. We show that the lower limb of the pH dependence curve results from differences in the pK_a values of two conserved histidine residues (His10 and His105) in the two states. The net proton affinity of His10 is about 50 times higher and that of His105 is 13 times higher in the D-state than in the S-state. The origin of the high limb of the D \rightleftharpoons S pH dependence remains to be determined. These results show that changes in proton inventory need to be taken into account in the steps in iron–sulfur cluster assembly and transfer that involve transitions of IscU between its S- and D-states.



Iron–sulfur (Fe–S) proteins are among the most ancient of macromolecules.¹ They are involved in various biochemical processes, including nitrogen fixation, metabolic catalysis, regulation of gene expression, and electron transfer.^{2–4} The major pathway for Fe–S cluster biosynthesis, the ISC pathway, is highly conserved across the many species in which it occurs.¹ Defects in this machinery underlie many human diseases and aging processes.^{5–8}

IscU (IscU1 and IscU2 in yeast; ISC1 in human) is a major player among the several proteins involved in the ISC pathway. IscU is the scaffold protein on which the Fe–S cluster is assembled and from which the Fe–S cluster is delivered to a receiver apoprotein. Structures of forms of IscU containing Zn²⁺ or [2Fe–2S] ligated have been determined by NMR spectroscopy⁹ and X-ray crystallography.^{10–14} However, studies from our laboratory have shown that IscU in the absence of metal or Fe–S cluster populates two distinct conformations that interchange on a subsecond time scale^{4,15,16} and interact differentially with other proteins involved in Fe–S cluster assembly and delivery.^{4,17,18} The S-state is structured, and the D-state lacks secondary structure¹⁷ but is not unfolded.¹⁹ In addition, N13–P14 and P100–P101, two peptidyl-prolyl peptide bonds that are *trans* in the S-state, become *cis* in the D-state.²⁰ We report here that the D \rightleftharpoons S equilibrium is pH-dependent, with the S-state favored at intermediate pH values and the D-state favored at high and low pH. NMR studies demonstrate that the transition at low pH is explained by differences in the pK_a values of two conserved histidine residues (H10 and H105) in the S- and D-states. The origin of the

transition at high pH remains to be determined. We postulate that IscU evolved these properties to match changes in proton inventory in the cluster assembly and transfer reactions.

MATERIALS AND METHODS

Protein Production and Purification. Unlabeled IscU samples were produced and purified as described previously.²¹ [U–¹⁵N]- and [U–¹³C, U–¹⁵N]-labeled samples of IscU protein were prepared according to procedures adapted from earlier studies.^{22,23} A colony of BL21 cells transformed with the pTrc 99A plasmid containing the IscU gene was used to inoculate 5 mL of TB liquid medium containing 100 μg/mL ampicillin. The cells were grown overnight at 37 °C, and a 100 μL of inoculum was transferred to 250 mL of TB liquid medium containing 100 μg/mL ampicillin. The culture was subsequently grown for 12 h at 37 °C.

Cells from this 250 mL culture were used to inoculate 1000 mL of M9 medium containing 100 μg/mL ampicillin and supplemented with 1 mL of vitamin solution,²¹ 1 g of ¹⁵NH₄Cl, and 4 g unlabeled glucose to produce [U–¹⁵N]-IscU. The culture was induced at an OD₆₀₀ of ≈1 by adding IPTG to a final concentration of 0.4 mM. Protein production was allowed to proceed for 12 h, after which cells were harvested and stored at –80 °C. For production of [U–¹³C, U–¹⁵N]-IscU, unlabeled glucose was substituted with 4 g of [U–¹³C]-D-glucose. For

Received: March 12, 2014

Revised: June 25, 2014

Published: July 23, 2014

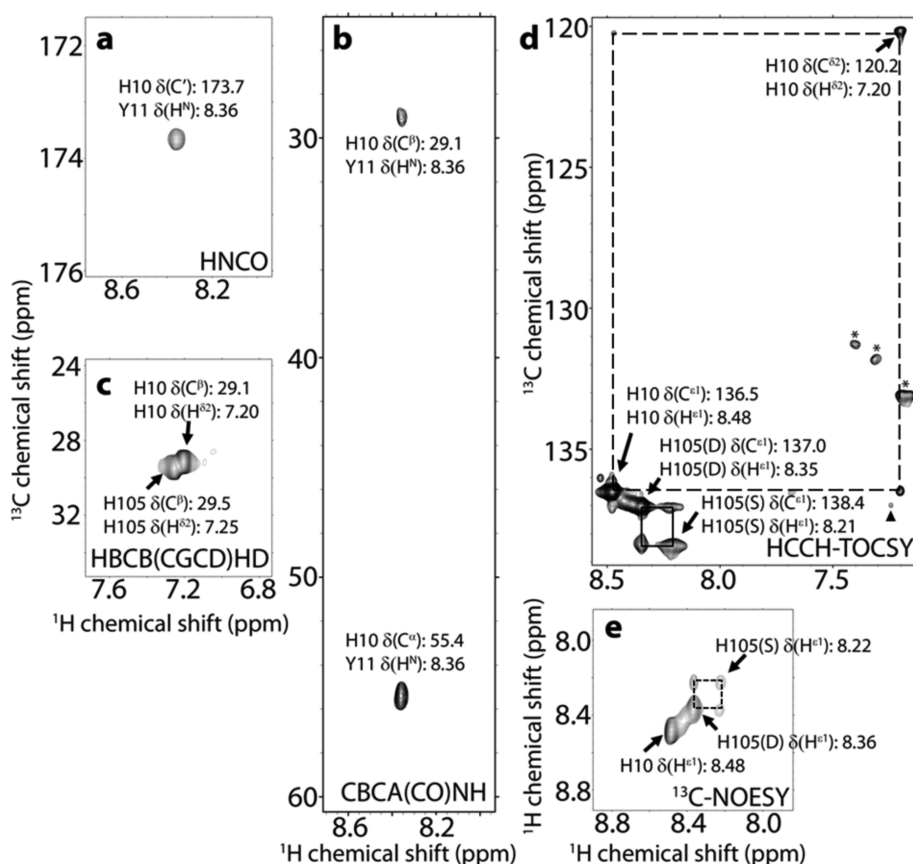


Figure 1. NMR spectra of [^{13}C , ^{15}N -His; ^{15}N -Tyr]-IscU used in assigning NMR signals to H10 and H105. Data were collected at pH 6.0 and 25 °C. Under these conditions, the only peaks assigned to H10 were from the D-state, whereas residue H105 exhibited peaks from both the S- and D-states (H105(S) and H105(D), respectively). (a) Because IscU contains only one H–Y dipeptide (that from H10–Y11), the single peak in the 2D HNCO spectrum is assigned to the connectivity between H10- $^{13}\text{C}'$ and Y11- $^1\text{H}^{\text{N}}$. (b) The two peaks observed in the 2D CBCA(CO)NH spectrum, which aligned with the signal assigned to Y11- $^1\text{H}^{\text{N}}$, provided the $^{13}\text{C}^{\alpha}$ and $^{13}\text{C}^{\beta}$ chemical shifts of H10. (c) The 2D HBCB(CGCD)HD spectrum served to extend the assignment from H10 $^{13}\text{C}^{\beta}$ to the side-chain $^1\text{H}^{\delta 2}$ of that residue. The other peak was then assigned to the $^{13}\text{C}^{\beta}$ – $^1\text{H}^{\delta 2}$ connectivity of H105. (d) The 2D aromatic HCCH-TOCSY spectrum showed the single-bond $^1\text{H}^{\delta 2}$ – $^{13}\text{C}^{\delta 2}$ and $^1\text{H}^{\epsilon 1}$ – $^{13}\text{C}^{\epsilon 1}$ connectivities from H10 as diagonal peaks connected by crosspeaks (dashed line). The $^1\text{H}^{\epsilon 1}$ – $^{13}\text{C}^{\epsilon 1}$ diagonal peak from H105(D) was observed. Although the $^1\text{H}^{\delta 2}$ – $^{13}\text{C}^{\delta 2}$ from H105(D) (seen in panel c) was missing because of the long mixing time of the pulse sequence, it was observed in a spectrum accumulated with a shorter mixing time (data not shown); a peak (labeled with a triangle) was seen corresponding to the H105(D) $^{13}\text{C}^{\epsilon 1}$ – $^1\text{H}^{\delta 2}$ connectivity. A peak was observed and assigned to H105(S) $^1\text{H}^{\epsilon 1}$ – $^{13}\text{C}^{\epsilon 1}$ by virtue of exchange crosspeaks (solid line) linking the signals from this residue in the two conformational states. The peaks marked by asterisks apparently correspond to aromatic residues that became partially labeled through scrambling of the histidine label. (e) The 2D aromatic ^{13}C -edited NOESY spectrum exhibited chemical exchange peaks linking (dashed line) the diagonal peaks at 8.22 and 8.36 ppm assigned, respectively, to H105(S) $^1\text{H}^{\epsilon 1}$ and H105(D) $^1\text{H}^{\epsilon 1}$.

production of [^{13}C , ^{15}N -His; ^{15}N -Tyr]-IscU, the M9 medium contained 100 $\mu\text{g}/\text{mL}$ ampicillin, 1 g/L unlabeled- NH_4Cl , 4 g/L unlabeled-glucose, 0.1 g/L [$\text{U}-^{13}\text{C}$, $\text{U}-^{15}\text{N}$]-histidine, and 0.17 g/L [$\text{U}-^{15}\text{N}$]-tyrosine. In order to further suppress scrambling of the labeled amino acids, the following amino acids were also added to the medium: 0.5 g/L alanine, 0.4 g/L arginine, 0.4 g/L aspartic acid, 0.05 g/L cystine, 0.4 g/L glutamine, 0.65 g/L glutamic acid, 0.55 g/L glycine, 0.23 g/L isoleucine, 0.23 g/L leucine, 0.42 g/L lysine hydrochloride, 0.25 g/L methionine, 0.13 g/L phenylalanine, 0.1 g/L proline, 2.1 g/L serine, 0.23 g/L threonine, and 0.23 g/L valine. Protein purification was conducted as described previously.^{21,22} The elution buffer for this step consisted of 50 mM Tris-HCl (pH 8.0), 1 mM DTT, 0.5 mM EDTA, and 150 mM NaCl. Fractions were analyzed by gel electrophoresis, and those appearing homogeneous were pooled, concentrated by ultrafiltration, frozen in liquid nitrogen, and stored at -80°C . The isotopic labeling efficiency was determined by mass spectrometry.

NMR Samples and pH Titrations. Unless otherwise noted, the NMR sample buffer contained 0.5 mM EDTA, 5 mM DTT, 10% D_2O , 50 μM DSS, and 50 μM NaN_3 . The concentration of [$\text{U}-^{15}\text{N}$]-IscU was 1 mM unless specified otherwise. DSS was used as an internal reference for all titration data. To adjust the pH value of the solution, 100 mM HCl or NaOH was added gradually to the IscU samples. The pH readings were recorded both before and after the NMR measurements. The average values of the two are reported.

NMR Data Collection. NMR data were collected at the National Magnetic Resonance Facility at Madison (NMRFAM) on Varian (Agilent) VNMRs spectrometers equipped with z-gradient cryogenic probes. DSS was used as an internal reference for all NMR chemical shift measurements.

Assignment of Histidine Signals. IscU has two histidine residues, H10, which is followed by Y11, and H105, which is followed by C106. The $^1\text{H}^{\epsilon 1}$ – $^{13}\text{C}^{\epsilon 1}$ peaks of the two histidine residues were assigned by reference to spectra of [^{13}C , ^{15}N -His; ^{15}N -Tyr]-IscU. We collected NMR data at pH 6.0 because we

found that the histidine backbone amide peaks broadened at higher pH values. The following steps led to the assignment of the $^1\text{H}^{\epsilon 1}-^{13}\text{C}^{\epsilon 1}$ peak from H10. (i) As expected, a single peak was found in the HNCO spectrum corresponding to the through-bond connectivity between H10 $^{13}\text{C}'$ and Y11 ^{15}N (Figure 1a). (ii) Two peaks were observed in the CBCA(CO)NH spectrum (Figure 1b). Both of these peaks share ^1H and ^{15}N frequencies with the single peak from the HNCO spectrum, showing that they originate from $^{13}\text{C}^{\beta}-^{13}\text{C}^{\alpha}$ of H10 and the $^{15}\text{N}-^1\text{H}$ Y11. (iii) Two peaks were observed in the HBCB(CGCD)HD spectrum, correlating $^{13}\text{C}^{\beta}$ with the $^1\text{H}^{\delta 2}$ of its side chain for each of the two histidine residues. Only one of these peaks aligns with the $^{13}\text{C}^{\beta}$ peak from the CBCA(CO)NH spectrum, indicating that this peak correlates $^{13}\text{C}^{\beta}$ of H10 with the $^1\text{H}^{\delta 2}$ of its side chain. By exclusion, the other peak of the HBCB(CGCD)HD spectrum corresponds to the $^1\text{H}^{\delta 2}$ of H105 (Figure 1c). (iv) The aromatic HCCH-TOCSY experiment showed cross-peaks correlating the $^1\text{H}^{\delta 2}-^{13}\text{C}^{\delta 2}$ signal assigned to H10 with a $^1\text{H}^{\epsilon 1}-^{13}\text{C}^{\epsilon 1}$ from the same residue, leading to the assignment of the $^1\text{H}^{\epsilon 1}-^{13}\text{C}^{\epsilon 1}$ peak from H10 (Figure 1d). The peaks from H105 were assigned by difference. Because the D-state of IscU dominates at pH 6, we concluded that these peaks arise from residues in the D-state. The ^{13}C -edited NOESY spectrum (Figure 1e) exhibited off-diagonal peaks connecting the peak assigned to H105 in D-state with a peak assigned to H105 in the S-state. Full cross-assignment of the peaks assigned to H10 and H105 in the S- and D-states was confirmed by a 2D $^1\text{H}-^{13}\text{C}$ zz-exchange spectrum obtained at pH 9.66 (Figure 2).

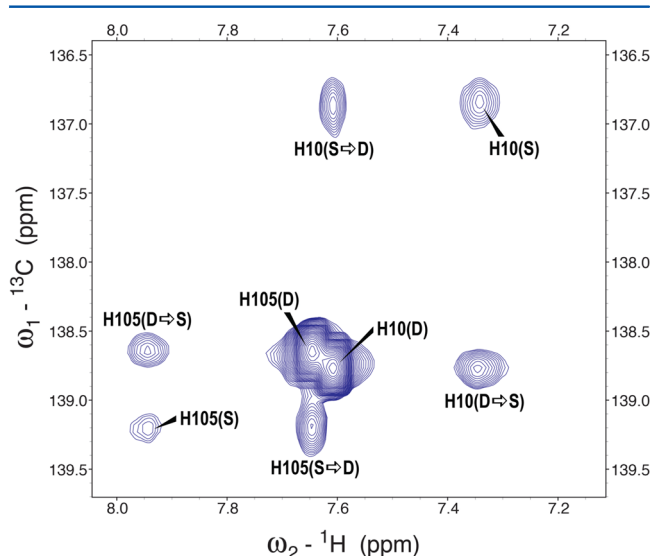


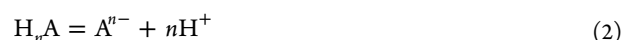
Figure 2. 2D $^1\text{H}-^{13}\text{C}$ zz-exchange NMR spectrum of $[^{13}\text{C}, ^{15}\text{N}\text{-His}; ^{15}\text{N}\text{-Tyr}]$ -IscU at pH 9.66 and 25 °C with 200 ms mixing time. Off-diagonal exchange peaks labeled H10(S \rightarrow D) and H10(D \rightarrow S) link the peaks assigned to H10(S) and H10(D), and off-diagonal exchange peaks labeled H105(S \rightarrow D) and H105(D \rightarrow S) link the peaks assigned to H105(S) and H105(D). Note that the peaks from the D-state are more intense than those from the S-state, indicating that the D-state predominates at this pH.

Conformational Equilibrium and Its pH Dependence.

The dissociation of the acid HA to the base A^- and a proton is represented by



In the case of n titratable groups, the equilibrium can be written as



In the two-state D \rightleftharpoons S equilibrium of IscU, the S-state is favored at intermediate pH and the D-state is favored at high and low pH. Here, we consider the transition at low pH. If we assume that n protonation–deprotonation steps are involved in the equilibrium with similar pK_a values, then we have

$$\text{pK}_a = \text{pH} - \frac{1}{n} \log \left(\frac{[\text{S}]}{[\text{D}]} \right) \quad (3)$$

where $[\text{S}]$ and $[\text{D}]$ are the relative population of the S- and D-states of the protein, respectively. This can be rearranged to

$$\log \left(\frac{[\text{S}]}{[\text{D}]} \right) = \text{pH}n - \text{pK}_an \quad (4)$$

We determined $[\text{S}]/[\text{D}]$ as a function of pH from the relative intensities of the Trp76 $^1\text{H}^{\epsilon 1}-^{15}\text{N}^{\epsilon 1}$ peaks assigned to the S- and D-states in ^{15}N -HSQC spectra (Figure 3). Fitting these data to eq 4 yielded the number n and average pK_a value for the titrating groups.

If the exchange of the titratable group falls under the fast exchange regime, then the chemical shifts average to

$$\delta = \delta_{\text{A}}\chi_{\text{A}} + \delta_{\text{HA}}\chi_{\text{HA}} \quad (5)$$

The averaged chemical shift (δ) becomes a weighted sum of the mole fraction of the acid (χ_{HA}) and its chemical shift (δ_{HA}) and the mole fraction of the conjugate base (χ_{A}) and its chemical shift (δ_{A}). Thus

$$\delta = \frac{\delta_{\text{A}} + \delta_{\text{HA}} \times 10^{(\text{pK}_a - \text{pH})}}{1 + 10^{(\text{pK}_a - \text{pH})}} \quad (6)$$

Fitting the chemical shifts and corresponding pH information to eq 6 yields the pK_a value of the titrating group as well as the chemical shifts in its protonated and deprotonated states.

RESULTS

pH Dependence of the IscU D \rightleftharpoons S Equilibrium.

Previous studies have shown that the S- and D-states of IscU give rise to different spectral signatures on the slow chemical shift time scale.^{4,15} Convenient signals for monitoring the S- and D-states are those from the side-chain $^{15}\text{N}^{\epsilon 1}-^1\text{H}^{\epsilon 1}$ of the single tryptophan residue W76. We acquired a series of 2D ^{15}N -HSQC spectra of $[\text{U}-^{15}\text{N}]$ -IscU at 25 °C at different pH values and used the relative intensities of the peaks assigned to the S- and D-states (Figure 3) to determine $[\text{S}]/([\text{S}] + [\text{D}])$. The pH range over which the equilibrium could be studied by 2D $^1\text{H}-^{15}\text{N}$ NMR was limited to a maximum of ~ 9.6 by the base-catalyzed exchange of the side-chain amide proton of W76 with protons from solvent water and a minimum of ~ 5.4 by protein precipitation at low pH. The results of this analysis (Figure 4a) showed that IscU transitions from the S-state to the D-state as the pH is lowered. A plot of $\log([\text{S}]/[\text{D}])$ vs pH (Figure 4b) yielded a straight line with a fitted slope of 0.50 and an intercept of 6.5. This result indicates that the D \rightleftharpoons S equilibrium is driven by the binding/release of two protons and suggests that the residues involved might be histidines. IscU contains two conserved histidines, H10 and H105.

Determination of the pK_a Values of the Histidine Residues of IscU. We collected $^1\text{H}-^{13}\text{C}$ HMQC spectra of

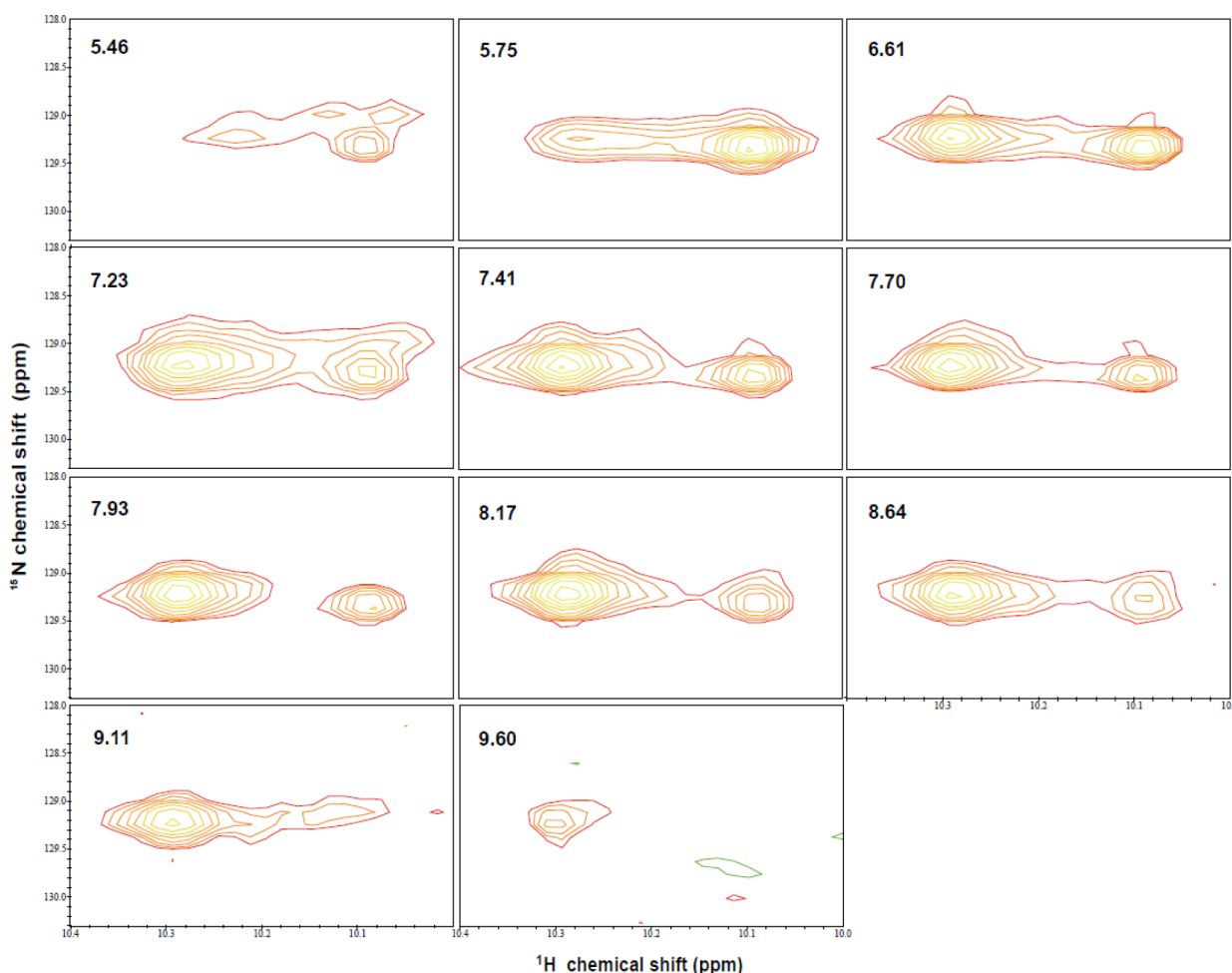


Figure 3. Tryptophan $^{15}\text{N}^{\epsilon 1}\text{--}^1\text{H}^{\epsilon 1}$ region of 2D ^{15}N -HSQC spectra of $[\text{U}\text{--}^{15}\text{N}]$ -IscU taken at 600 MHz (^1H) at the pH values indicated in each panel. The NMR sample contained 1 mM IscU, 0.5 mM EDTA, 5 mM DTT, 150 mM NaCl, 10% $\text{D}_2\text{O}/90\%$ H_2O , 50 μM DSS, and 50 μM NaN_3 . Signals were broadened and lost intensity at high pH as the result of amide hydrogen exchange with solvent.

^{13}C , ^{15}N -His; ^{15}N -Tyr]-IscU at 25 °C as a function of pH, which enabled us to track the positions of the $^1\text{H}^{\epsilon 1}\text{--}^{13}\text{C}^{\epsilon 1}$ crosspeaks from H10 and H105 (Figure 5). The ^1H chemical shifts of these crosspeaks are plotted as a function of pH in Figure 6a, and the ^{13}C chemical shifts are plotted in Figure 6b. The histidine peaks assigned to the D-state yielded titration curves with fitted pK_a values of 7.01 (from ^1H shifts) and 6.99 (from ^{13}C shifts) for H10(D) and 6.32 (from ^1H shifts) and 6.26 (from ^{13}C shifts) for H105(D) (Table 1). Complete titration curves could not be determined for the histidine peaks assigned to the S-state because the signals lost intensity as the pH was lowered as a consequence of $\text{S} \rightarrow \text{D}$ conversion and could not be followed below pH 6. Nevertheless, the upper bounds of the pK_a values could be estimated for H10(S) as 5.6 from the pH dependence of its $^1\text{H}^{\epsilon 1}$ signal and for H105(S) as 5.5 from the pH dependence of its $^1\text{H}^{\epsilon 1}$ signal and 5.3 from the pH dependence of its $^{13}\text{C}^{\epsilon 1}$ signal. The peak assigned to $^{13}\text{C}^{\epsilon 1}$ of H10(S) (Figure 6b) has an anomalous chemical shift and exhibited a small pH dependent shift with a midpoint of pH 7.9. This small shift in the opposite direction to that expected for titration of H10(S) itself must represent a spectroscopic shift resulting from protonation/deprotonation of some other group.

We confirmed the results for the D-state by carrying out the titration at 45 °C, where the D-state predominates (spectra not

shown). The pK_a values determined for H10(D) and H105(D) from the pH dependence of His $^1\text{H}^{\epsilon 1}\text{--}^{13}\text{C}^{\epsilon 1}$ signals in $^1\text{H}\text{--}^{13}\text{C}$ HMQC spectra of $[\text{U}\text{--}^{13}\text{C}]$ -IscU were very similar to those obtained at 25 °C (Table 1).

We determined pH dependence of the $\text{D} \rightleftharpoons \text{S}$ equilibrium from the H10(S)/H10(D) and H105(S)/H105(D) $^1\text{H}^{\epsilon 1}\text{--}^{13}\text{C}^{\epsilon 1}$ peak intensities in $^1\text{H}\text{--}^{13}\text{C}$ HMQC spectra of ^{13}C , ^{15}N -His; ^{15}N -Tyr]-IscU collected at various pH values (Figure 7). In contrast to the data from the $^{15}\text{N}^{\epsilon 1}\text{--}^1\text{H}^{\epsilon 1}$ signal of W76 (Figure 4a), a $\text{S} \rightarrow \text{D}$ shift was observed at high pH.

DISCUSSION

Previous studies have shown that IscU exists in equilibrium between two different conformational states, a more structured state (S) and a more dynamic state (D) that lacks secondary structure⁴ but is not unfolded in that it stabilizes two *cis* peptidyl-prolyl peptide bonds that are *trans* in the S-state.²⁰ Results presented here show that the $\text{D} \rightleftharpoons \text{S}$ equilibrium is pH-dependent, with the S-state predominant around pH 7 and the D-state stabilized at high and low pH (Figure 7). The high pH transition observed in $^1\text{H}\text{--}^{13}\text{C}$ data was missed in the $^1\text{H}\text{--}^{15}\text{N}$ NMR data (Figures 3 and 4a). This can be explained if the rate of exchange of the W76 $^1\text{H}^{\epsilon 1}$ with solvent is much higher in the D-state than in the S-state, as would result from higher solvent accessibility of W76 in the D-state. From the pH dependence of

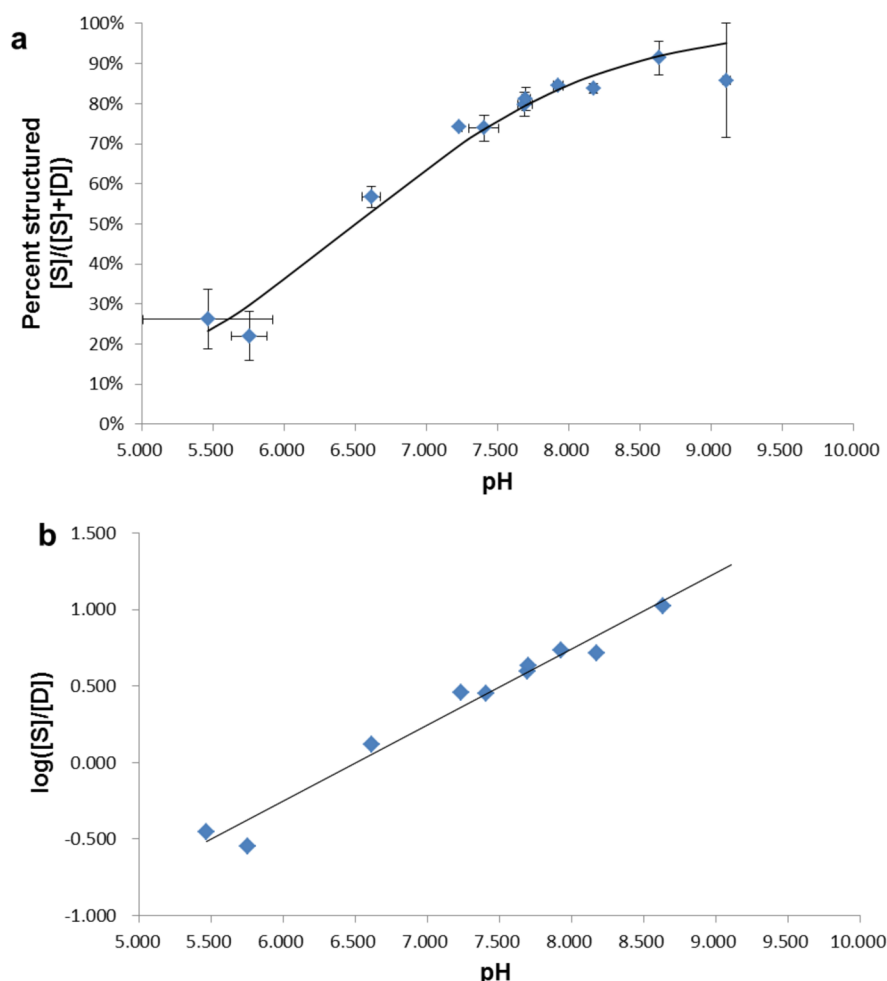


Figure 4. pH dependence of relative population of IscU conformers derived from the relative intensities of the signals assigned to W76 $^1\text{H}^{\epsilon 1}$ – $^{15}\text{N}^{\epsilon 1}$ shown in Figure 3. (a) Percentage of structured protein, $[S]/([S] + [D])$, plotted as a function of pH. (b) Log–log plot of $[S] = \text{A}^-$ and $[D] = \text{HA}$ vs pH used to determine the number of protons added (2.02).

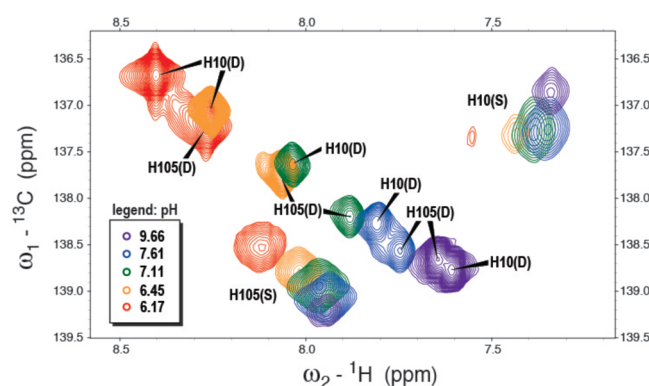


Figure 5. Overlay of 2D ^1H – ^{13}C -HMQC spectra of $[^{13}\text{C}, ^{15}\text{N}\text{-His}; ^{15}\text{N}\text{-Tyr}]\text{-IscU}$ taken at 600 MHz (^1H) at 25 °C and at five different pH values (color coded). The NMR sample contained 1 mM IscU, 0.5 mM EDTA, 5 mM DTT, 150 mM NaCl, 10% D_2O , 50 μM DSS, and 50 μM NaN_3 . Only the histidine $^1\text{H}^{\epsilon 1}$ – $^{13}\text{C}^{\epsilon 1}$ region is shown.

the high pH limb, we infer that the $\text{S} \rightarrow \text{D}$ transition involves a decrease in the proton affinity of one or more cysteine residues. Confirmation of this will require selective labeling of the cysteine residues. The plot of $\log([S]/[D])$ vs pH (Figure 4b) indicated the involvement of two protonation/deprotonation steps in the lower limb. By following the pH dependence of

chemical shifts of signals assigned to the two conserved histidine residues (H10 and H105) in the S- and D-states, we determined their pK_a values. In the D-state, H10 and H105 titrate with relatively normal pK_a values of 7.0 and 6.5, respectively (Table 1). However, in the S-state, both histidine side chains have abnormally low pK_a values. Although full titration curves could not be determined accurately for H10 and H105 in the S-state, we estimated the upper limits for their pK_a values as 5.3 and 5.6, respectively, from the average of their fitted values in Table 1. The minimum change in pK_a value resulting from the $\text{S} \rightarrow \text{D}$ transition was found to be 1.7 pH units (7.0–5.3) for H10 and 1.1 pH units (6.5–5.4) for H105. This indicates that the $\text{S} \rightarrow \text{D}$ transition increases the proton affinity at H10 by a factor of ≥ 50 and at H105 by a factor of ≥ 13 . In principle, the pH at which $\log([S]/[D]) = 0$ (6.5 from Figure 4b) should be the mean of the average pK_a values for the two residues (H10 and H105) in their S- and D-states: $(7.0 + 5.3)/2 + (6.5 + 5.4)/2 = 6.1$ from Table 1. The agreement, although not ideal, is likely within experimental error given the neglect of the high pH limb in analysis of the pH dependence of $\text{S} \rightleftharpoons \text{D}$. Because of peak overlap, we were unable to obtain a sufficient number of points at high pH to analyze both the high and low pH limbs from the ^1H – ^{13}C peak intensities (Figure 7).

H105 appears to be conserved absolutely in IscU from all organisms, and H10 is conserved absolutely in all organism

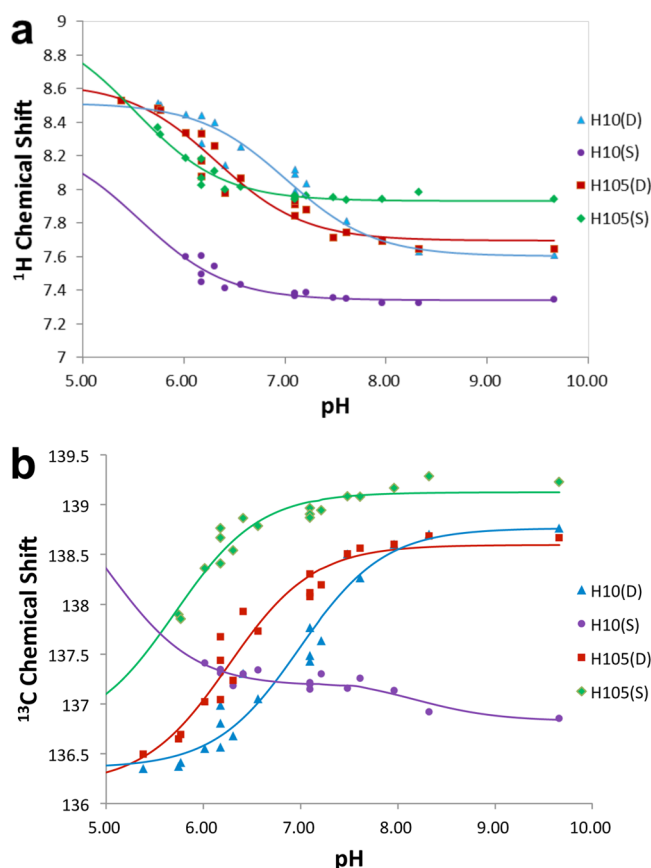


Figure 6. Plots of data from 2D ^1H – ^{13}C HMQC spectra of [^{13}C , ^{15}N -His; ^{15}N -Tyr]-IscU collected at 600 MHz (^1H) as a function of pH. The probe temperature was regulated at 25 °C. (a) Chemical shifts of crosspeaks assigned to the imidazole $^1\text{H}^{\text{e1}}$ – $^{13}\text{C}^{\text{e1}}$ of His10 and His105 in the S- and D-states. (b) Chemical shifts of crosspeaks assigned to the imidazole $^{13}\text{C}^{\text{e1}}$ of H10 and H105 in the S- and D-states.

classes with the exception of some α -proteobacteria.¹⁵ H10 in the S-state exhibits anomalous chemical shifts and titration behavior. The H10(S) $^{13}\text{C}^{\text{e1}}$ peak exhibits a pH_{mid} at ~8.2 that may correspond to the protonation/deprotonation step(s) responsible for the S \rightarrow D conversion at high pH. When H10(S) accepts a proton at low pH, as inferred from the chemical shift of the H10(S) $^1\text{H}^{\text{e1}}$ peak, the H10(S) $^{13}\text{C}^{\text{e1}}$ peak shifts in a direction opposite to normal. The PACSY database,²⁴ which enables searches of structures that correspond to NMR chemical shifts, yielded a match for the unusual IscU H10(S)

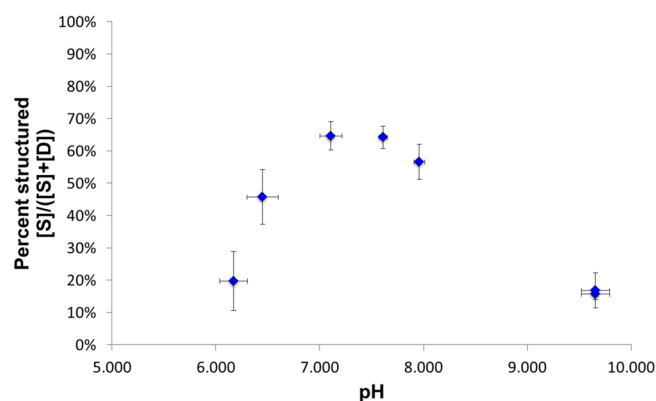


Figure 7. Percentage of structured protein, $[S]/([S] + [D])$, plotted as a function of pH, as determined from the intensities of the $^1\text{H}^{\text{e1}}$ – $^{13}\text{C}^{\text{e1}}$ of peaks from His10 and His105 in 2D ^1H – ^{13}C HMQC spectra of [^{13}C , ^{15}N -His; ^{15}N -Tyr]-IscU collected at 600 MHz (^1H) as a function of pH. $[S]/([S] + [D])$ was obtained from the average intensities of the peaks from H10(D) and H105(D) and H10(S) and H105(S).

$^{13}\text{C}^{\text{e1}}$ chemical shift of 137 ppm at pH 8.5. The match was to H111 of an ATPase, a histidine residue largely buried in a hydrophobic cavity near a lysine residue (BMRB 5576; PDB ID: 1mo8).²⁵ Although the position of H10 was not defined in the NMR structure of the S-state of IscU (PDB ID: 2l4x),¹⁶ the imidazole ring of residues homologous to H10 were found buried adjacent to a short α -helix in the X-ray structures of [2Fe–2S]-IscU (PDB ID: 2z7e)¹² and the IscU–IscS complex (PDB ID: 3lvi)²⁶ and the NMR structure of Zn-bound SufU (PDB ID: 2azh).²⁷

What may explain the evolutionary conservation of these two residues of IscU that have very different chemical properties in the two conformational states? IscU, as the scaffold protein for Fe–S cluster assembly and delivery, is a hub protein that interacts with several different partner proteins in this process. Results from our laboratory have shown that the cysteine desulfurase (IscS)⁴ and the Hsp70-type chaperone in its ADP-bound state (HscA:ADP)¹⁷ each bind preferentially to the D-state of IscU, whereas the iron-delivery protein (IscX)¹⁸ and the Hsp40-type cochaperone (HscB)^{22,17} each bind preferentially to the S-state of IscU. Thus, in the course of Fe–S cluster biosynthesis, IscU may potentially interconvert between its D- and S-states six times: (S) predominant state of free IscU (1) \rightarrow (D) IscU–IscS (first sulfur transfer) (2) \rightarrow (S) IscU–IscX (first iron transfer) (3) \rightarrow (D) IscU–IscS (second sulfur

Table 1. Results from Fitting of pH Dependence of NMR Chemical Shifts from 2D ^1H – ^{13}C Spectra of [^{13}C , ^{15}N -His; ^{15}N -Tyr]-IscU and Attributed to Protonation/Deprotonation of the Histidine Residues^a

sample	atom	H10 (D-state)				H105 (D-state)			
		$\delta(\text{HA})$	$\delta(\text{A}^-)$	pK_{a}	R^2 value	$\delta(\text{HA})$	$\delta(\text{A}^-)$	pK_{a}	R^2 value
IscU at 25 °C	^{13}C	136	139	6.99	0.952	136	139	6.47	0.968
	^1H	8.52	7.60	7.01	0.948	8.63	7.64	6.52	0.987
IscU at 45 °C	^{13}C	137	139	7.1	0.996	137	139	6.58	0.967
	^1H	8.49	7.62	7	0.995	8.48	7.66	6.44	0.986
sample	atom	H10 (S-state)				H105 (S-state)			
		$\delta(\text{HA})$	$\delta(\text{A}^-)$	pK_{a}	R^2 value	$\delta(\text{HA})$	$\delta(\text{A}^-)$	pK_{a}	R^2 value
IscU at 25 °C	^{13}C	139	137	5.0	0.621	134	139	5.3	0.920
	^1H	8.30	7.34	5.6	0.842	9.00	7.93	5.52	0.920

^aThe titration data were fitted to eq 6.

transfer) (4) \rightarrow (S) IScU–IsC_X (second iron transfer and cluster assembly) followed by formation of IScU[2Fe–2S]–HscB (5) \rightarrow (D) IScU–HscA(ADP) (6) \rightarrow (S) free IScU.

Many of the processes taking place in Fe–S cluster assembly and delivery involve protonation and deprotonation steps. Thus, it is tempting to speculate how these might be coupled to the changes in proton affinity of IScU accompanying $S \rightleftharpoons D$ interconversion. The coupling could be direct or through chains of water molecules. Because the binding of metal ions, such as Zn^{2+} or Fe^{2+} , has been shown to shift the $S \rightleftharpoons D$ equilibrium completely to the S-state,⁴ the D-state appears to have a low affinity for metals. NMR studies have shown that the cysteine desulfurase, IscS, binds preferentially to the D-state of IScU.⁴ This interaction minimizes metal binding to IScU and thus ensures that its cysteine residues are unligated and available to pick up the sulfur atom generated by IscS through its catalysis of the conversion of L-cysteine to L-alanine. Protonation of the metal ligand H105 would serve to inhibit metal binding. The increased proton affinity of IScU could assist in the deprotonation of the cysteine S^γ of IScU that picks up sulfur from IscS.

The S-state favored by interaction with IscX:Fe²⁺¹⁸ puts IScU into the conformation that binds metal ions. The two protons released upon the D \rightarrow S conversion may serve to protonate the IscX side chains that ligate Fe²⁺ and catalyze transfer of the iron ion to IScU. The S-state is further stabilized upon formation of the Fe–S cluster. Once deprotonated, H105 is in the state to bind one of the iron atoms of the cluster, as observed in the X-ray structure of [2Fe–2S]–IscU.¹²

Fe–S cluster transfer first involves formation of the HscB–IscU[2Fe–2S]–HscA(ATP) complex. We have postulated that the attack of one, or probably two, cysteine side chains of the acceptor protein on the iron atoms of the cluster bound to IScU serves to trigger the cascade of reactions leading to cluster transfer.¹⁹ The attack of two cysteine –SH groups would liberate two protons; these could be transferred to the displaced side chains of IScU, most likely those of H105 and one of the cysteines. Protonation of H105 would favor S \rightarrow D conversion, and the ensuing conformational change could lead to activation of the ATPase, converting HscA:ATP to HscA:ADP. ATP hydrolysis liberates a proton that could be picked up by H10. HscA:ADP binds preferentially to the D-state of IScU,¹⁷ and this interaction would ensure complete release of the cluster to the acceptor protein. Finally, exchange of bound ADP with ATP regenerates HscA:ATP, which releases IScU and allows it to regain its predominant S-state.

Our results clearly show that the histidine residues of IScU have very different proton affinities in its D- and S-states. As noted above, additional experiments will be required to determine the origin of the S \rightarrow D shift at high pH. If, as suspected, the shift arises from decreased proton affinity of cysteine residue(s), then this would point to higher cysteine reactivity in the D-state than that in the S-state.

AUTHOR INFORMATION

Corresponding Author

*E-mail: markley@nmrfam.wisc.edu. Phone: +1 608-263-9349. Fax: +1 608-262-3759.

Present Address

[†]Max Planck Institute for Biophysical Chemistry, Göttingen, Germany.

Funding

This work was supported by National Institutes of Health (NIH) grants R01 GM58667 and U01 GM94622 in collaboration with the National Magnetic Resonance Facility at Madison, which is supported by NIH grant P41GM66326. Equipment was purchased with funds from the University of Wisconsin–Madison, the NIH (P41RR02301, P41GM66326, S10RR02781, S10RR08438, S10RR023438, S10RR025062, and S10RR029220), the NSF (DMB-8415048, OIA-9977486, and BIR-9214394), and the USDA.

Notes

The authors declare no competing financial interest.

ACKNOWLEDGMENTS

The authors thank NMRFAM staff members for assistance with NMR instrumentation.

ABBREVIATIONS

[¹³C,¹⁵N-His; ¹⁵N-Tyr], selectively histidine and tyrosine labeled with ¹³C/¹⁵N and ¹⁵N, respectively; [U–¹³C], uniformly ¹³C-labeled; [U–¹⁵N], uniformly ¹⁵N-labeled; [U–¹³C, U–¹⁵N], uniformly ¹³C/¹⁵N-labeled; DSS, 4,4-dimethyl-4-silapentane-1-sulfonic acid; DTT, dithiothreitol; HscA, Hsp70-type chaperone protein; HMQC, heteronuclear multiple-quantum correlation; HSQC, heteronuclear single-quantum correlation; IscS, cysteine desulfurase; IScU, scaffold protein for iron–sulfur cluster biosynthesis; NMR, nuclear magnetic resonance; NOESY, nuclear Overhauser enhancement spectroscopy; TOCSY, total correlated spectroscopy

REFERENCES

- (1) Lill, R. (2009) Function and biogenesis of iron–sulfur proteins. *Nature* 460, 831–838.
- (2) Ayala-Castro, C., Saini, A., and Outten, F. W. (2008) Fe–S cluster assembly pathways in bacteria. *Microbiol. Mol. Biol. Rev.* 72, 110–125.
- (3) Johnson, M. K. (1998) Iron–sulfur proteins: new roles for old clusters. *Curr. Opin. Chem. Biol.* 2, 173–181.
- (4) Kim, J. H., Tonelli, M., and Markley, J. L. (2012) Disordered form of the scaffold protein IScU is the substrate for iron–sulfur cluster assembly on cysteine desulfurase. *Proc. Natl. Acad. Sci. U.S.A.* 109, 454–459.
- (5) Rouault, T. A., and Tong, W. H. (2008) Iron–sulfur cluster biogenesis and human disease. *Trends Genet.* 24, 398–407.
- (6) Sheftel, A., Stehling, O., and Lill, R. (2010) Iron–sulfur proteins in health and disease. *Trends Endocrinol. Metab.* 21, 302–314.
- (7) Shi, Y., Ghosh, M. C., Tong, W. H., and Rouault, T. A. (2009) Human ISD11 is essential for both iron–sulfur cluster assembly and maintenance of normal cellular iron homeostasis. *Hum. Mol. Genet.* 18, 3014–3025.
- (8) Campuzano, V., Montermini, L., Molto, M. D., Pianese, L., Cossee, M., Cavalcanti, F., Monros, E., Rodius, F., Duclos, F., Monticelli, A., Zara, F., Canizares, J., Koutnikova, H., Bidichandani, S. I., Gellera, C., Brice, A., Trouillas, P., De Michele, G., Filla, A., De Frutos, R., Palau, F., Patel, P. I., Di Donato, S., Mandel, J. L., Cocozza, S., Koenig, M., and Pandolfo, M. (1996) Friedreich's ataxia: autosomal recessive disease caused by an intronic GAA triplet repeat expansion. *Science* 271, 1423–1427.
- (9) Ramelot, T. A., Cort, J. R., Goldsmith-Fischman, S., Kornhaber, G. J., Xiao, R., Shastry, R., Acton, T. B., Honig, B., Montelione, G. T., and Kennedy, M. A. (2004) Solution NMR structure of the iron–sulfur cluster assembly protein U (IscU) with zinc bound at the active site. *J. Mol. Biol.* 344, 567–583.
- (10) Shimomura, Y., Kamikubo, H., Nishi, Y., Masako, T., Kataoka, M., Kobayashi, Y., Fukuyama, K., and Takahashi, Y. (2007)

Characterization and crystallization of an IscU-type scaffold protein with bound [2Fe–2S] cluster from the hyperthermophile *Aquifex aeolicus*. *J. Biochem.* 142, 577–586.

(11) Wu, G., Mansy, S. S., Wu, S. P., Surerus, K. K., Foster, M. W., and Cowan, J. A. (2002) Characterization of an iron–sulfur cluster assembly protein (ISU1) from *Schizosaccharomyces pombe*. *Biochemistry* 41, 5024–5032.

(12) Shimomura, Y., Wada, K., Fukuyama, K., and Takahashi, Y. (2008) The asymmetric trimeric architecture of [2Fe–2S] IscU: implications for its scaffolding during iron–sulfur cluster biosynthesis. *J. Mol. Biol.* 383, 133–143.

(13) Unciuleac, M. C., Chandramouli, K., Naik, S., Mayer, S., Huynh, B. H., Johnson, M. K., and Dean, D. R. (2007) In vitro activation of apo-aconitase using a [4Fe–4S] cluster-loaded form of the IscU [Fe–S] cluster scaffolding protein. *Biochemistry* 46, 6812–6821.

(14) Foster, M. W., Mansy, S. S., Hwang, J., Penner-Hahn, J. E., Surerus, K. K., and Cowan, J. A. (2000) A mutant human IscU protein contains a stable [2Fe–2S](2+) center of possible functional significance. *J. Am. Chem. Soc.* 122, 6805–6806.

(15) Kim, J. H., Füzéry, A. K., Tonelli, M., Ta, D. T., Westler, W. M., Vickery, L. E., and Markley, J. L. (2009) Structure and dynamics of the iron–sulfur cluster assembly scaffold protein IscU and its interaction with the cochaperone HscB. *Biochemistry* 48, 6062–6071.

(16) Kim, J. H., Tonelli, M., Kim, T., and Markley, J. L. (2012) Three-dimensional structure and determinants of stability of the iron–sulfur cluster scaffold protein IscU from *Escherichia coli*. *Biochemistry* 51, 5557–5563.

(17) Kim, J. H., Tonelli, M., Frederick, R. O., Chow, D. C., and Markley, J. L. (2012) Specialized Hsp70 chaperone (HscA) binds preferentially to the disordered form, whereas J-protein (HscB) binds preferentially to the structured form of the iron–sulfur cluster scaffold protein (IscU). *J. Biol. Chem.* 287, 31406–31413.

(18) Kim, J. H., Bothe, J. R., Frederick, R. O., Holder, J. C., and Markley, J. L. (2014) Role of IscX in iron–sulfur cluster biogenesis in *Escherichia coli*. *J. Am. Chem. Soc.* 136, 7933–7942.

(19) Markley, J. L., Kim, J. H., Dai, Z., Bothe, J. R., Cai, K., Frederick, R. O., and Tonelli, M. (2013) Metamorphic protein IscU alternates conformations in the course of its role as the scaffold protein for iron–sulfur cluster biosynthesis and delivery. *FEBS Lett.* 587, 1172–1179.

(20) Dai, Z., Tonelli, M., and Markley, J. L. (2012) Metamorphic protein IscU changes conformation by cis–trans isomerizations of two peptidyl-prolyl peptide bonds. *Biochemistry* 51, 9595–9602.

(21) Hoff, K. G., Silberg, J. J., and Vickery, L. E. (2000) Interaction of the iron–sulfur cluster assembly protein IscU with the Hsc66/Hsc20 molecular chaperone system of *Escherichia coli*. *Proc. Natl. Acad. Sci. U.S.A.* 97, 7790–7795.

(22) Füzéry, A. K., Tonelli, M., Ta, D. T., Cornilescu, G., Vickery, L. E., and Markley, J. L. (2008) Solution structure of the iron–sulfur cluster cochaperone HscB and its binding surface for the iron–sulfur assembly scaffold protein IscU. *Biochemistry* 47, 9394–9404.

(23) Bonomi, F., Iametti, S., Morleo, A., Ta, D., and Vickery, L. E. (2008) Studies on the mechanism of catalysis of iron–sulfur cluster transfer from IscU[2Fe2S] by HscA/HscB chaperones. *Biochemistry* 47, 12795–12801.

(24) Lee, W., Yu, W., Kim, S., Chang, I., Lee, W., and Markley, J. L. (2012) PACSY, a relational database management system for protein structure and chemical shift analysis. *J. Biomol. NMR* 54, 169–179.

(25) Hilge, M., Siegal, G., Vuister, G., Guentert, P., Gloor, S., and Abrahams, J. (2003) ATP-induced conformational changes of the nucleotide-binding domain of Na,K-ATPase. *Nat. Struct. Biol.* 10, 468–474.

(26) Shi, R., Proteau, A., Villarroja, M., Moukadiri, I., Zhang, L., Trempe, J. F., Matte, A., Armengod, M. E., and Cygler, M. (2010) Structural basis for Fe–S cluster assembly and tRNA thiolation mediated by IscS protein–protein interactions. *PLoS Biol.* 8, 18.

(27) Kornhaber, G. J., Swapna, G. V. T., Ramelot, T. A., Cort, J. R., Aramini, J. M., Kennedy, M. A., and Montelione, G. T. (2011) Solution NMR Structure of Zn-Ligated Fe–S Cluster Assembly

Scaffold Protein SufU from *Bacillus subtilis*. PDB entry 2azh, DOI:10.2210/pdb2azh/pdb.